

Study of enantioselective metolachlor adsorption by activated carbons

Alicia Gomis-Berenguer^{*a}, Isabelle Laidin^b, Sophie Renoncial^b and Benoît Cagnon^{*a}

^aInterfaces, Confinement, Matériaux et Nanostructures-ICMN, UMR 7374-CNRS, Université d'Orléans, 1B, rue de la Férellerie, 45071 Orléans Cedex 2, France.

^bJACOBI carbons, 15 Route de Foëcy, 18100 Vierzon, France.

ELECTRONIC SUPPLEMENTARY INFORMATION

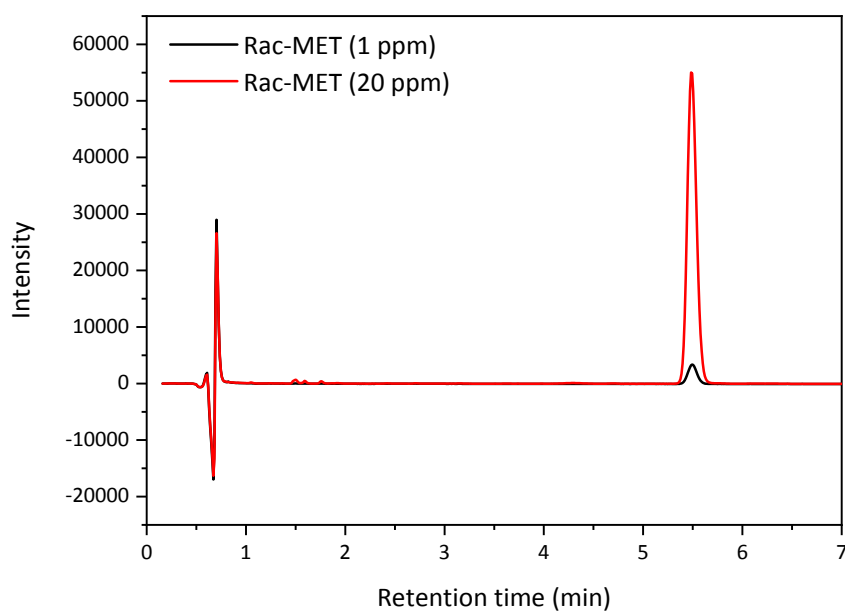


Figure S1. Example of chromatogram obtained for Rac-Metolachlor (1 and 20 ppm) at 230 nm.

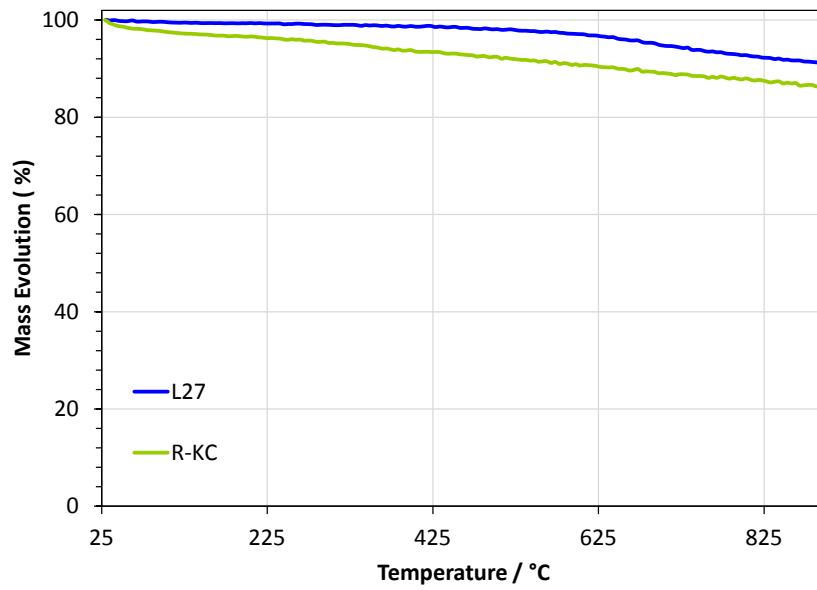


Figure S2. Thermogravimetric profile of R-KC and L27 adsorbents obtained under Ar flow (50 mL/min, 10 °C/min).

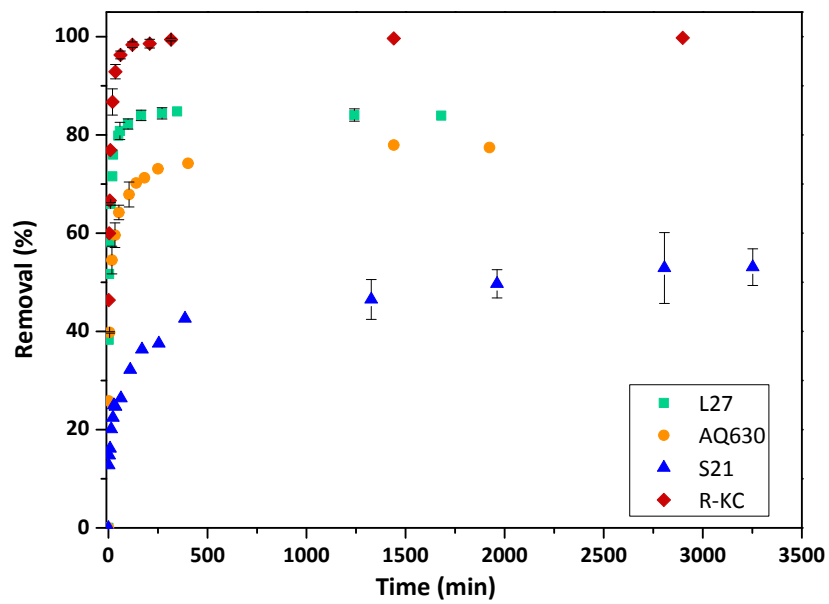


Figure S3. Evolution of Rac-Metolachlor adsorption in removal percentage as a function of the contact time at 25 °C for the four adsorbents. The error bars represent the standard deviation.

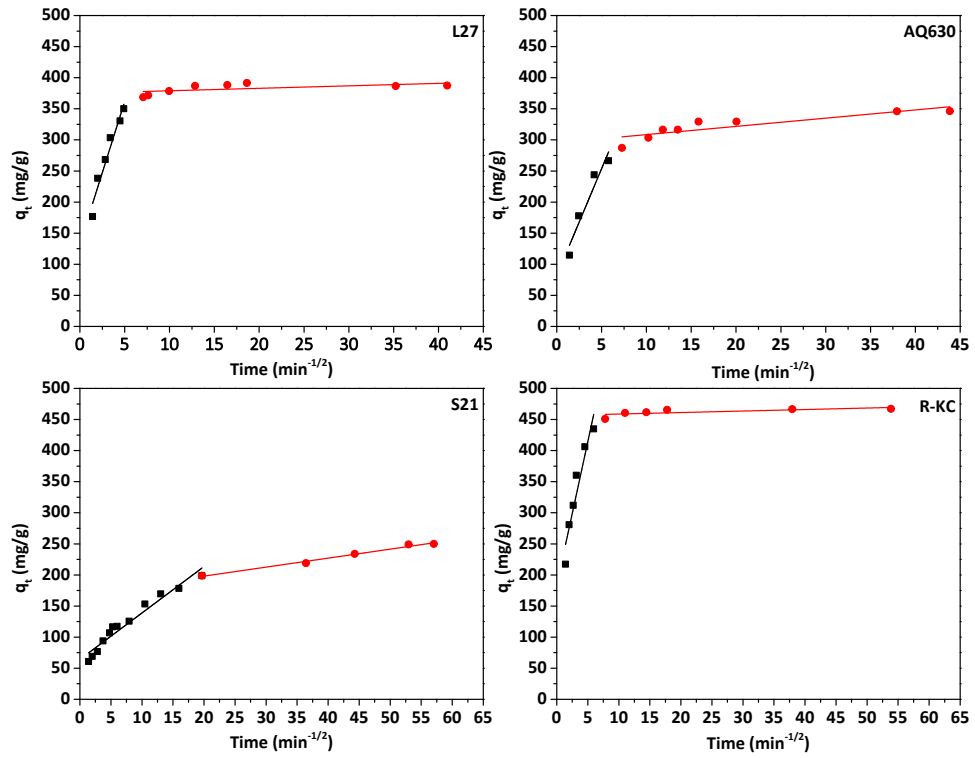


Figure S4. Intraparticle diffusion for Rac-Metolachlor on L27, AQ630, S21 and R-KC.

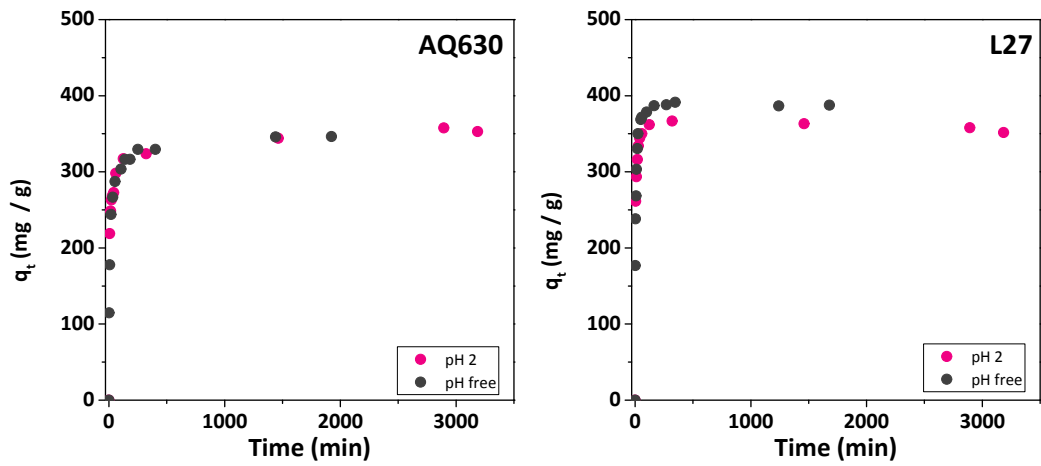


Figure S5. Adsorption kinetics of Rac-Metolachlor on AQ630 (left) and L27 (right) in aqueous solution at pH free and pH 2.

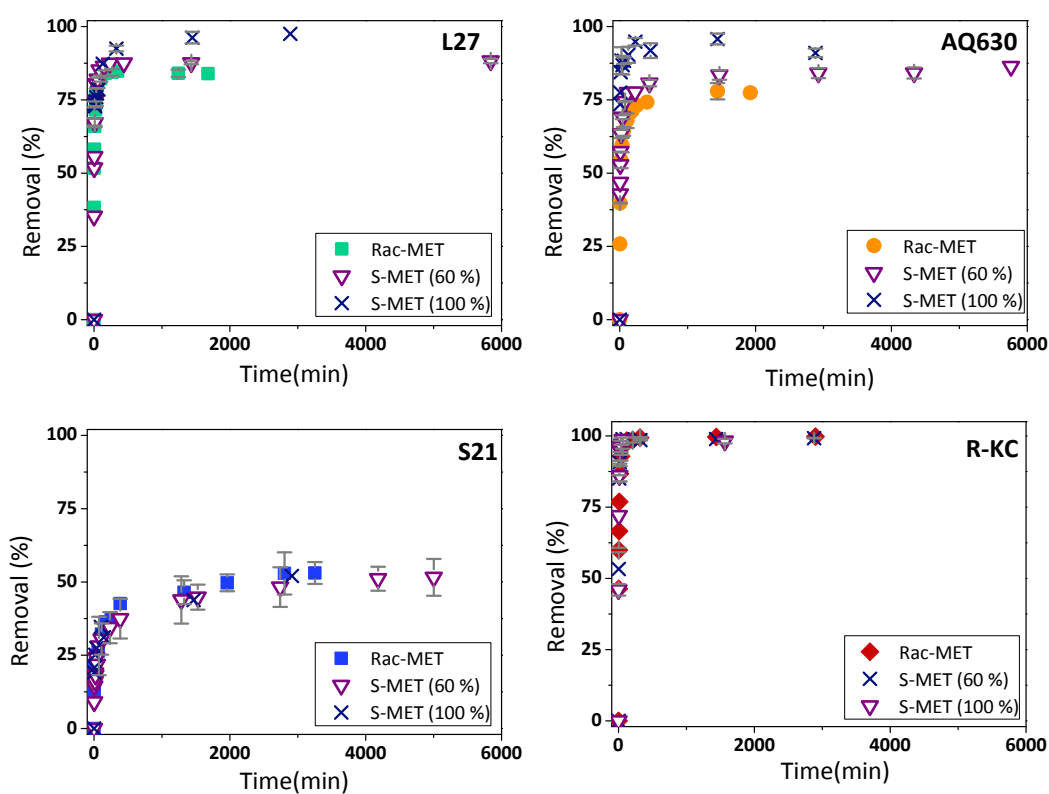


Figure S6. Evolution of Rac-Metolachlor, S-Metolachlor (60 %) and S-Metolachlor (100 %) removal efficiency as a function of the contact time at 25 °C for the four adsorbents. The error bars represent the standard deviation. adsorption in removal percentage.

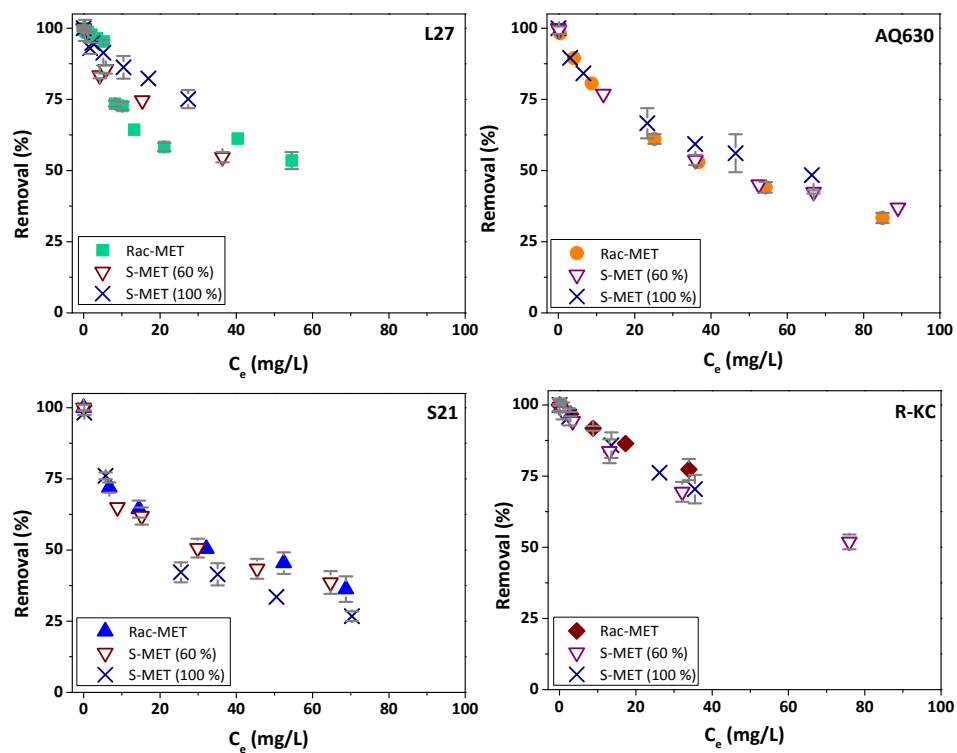


Figure S7. Experimental efficiency removal percentage of Rac-Metolachlor, S-Metolachlor (60 %) and S-Metolachlor (100 %) at 25 °C for the four adsorbents. The error bars represent the standard deviation

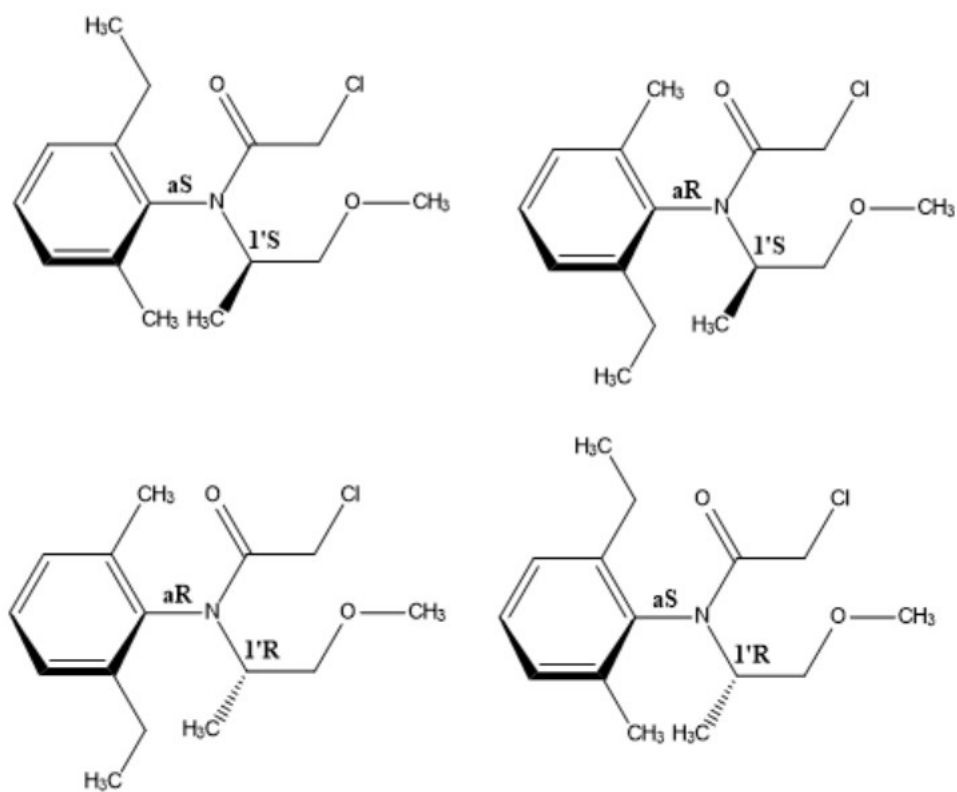


Figure S8. Atropisomers of Metolachlor molecule.